Effects of an annular solar eclipse on montane streamwater quality in New Mexico, USA

Robert R. Parmenter[1,2,4], Anna R. Grendys[1,5], David W. Pittenger[1,6], and Gregory D. McCurdy[3,7]

[1]United States National Park Service, Valles Caldera National Preserve, Jemez Springs, New Mexico USA
[2]Department of Biology, University of New Mexico, Albuquerque, New Mexico USA
[3]Desert Research Institute, Reno, Nevada USA

Abstract: We studied the atmospheric and streamwater-quality responses to the 14 October 2023 annular solar eclipse in 7 streams in the Jemez River basin of northern New Mexico, USA. Study sites ranged from 1st-order streams to the 4th-order Jemez River. During the eclipse, across 7 weather stations, we recorded a mean decrease of 92% insolation, a 6.7°C decline in air temperature, a 16.2% increase in relative humidity, and a 1.2 m/s drop in mean wind speed. During the eclipse, we observed distinct, small-magnitude, short-duration changes in the diel cycles of stream temperatures (mean decline of 0.67°C across 7 streams), dissolved O_2 (decline of 0.22 mg/L in 5 streams showing responses), and pH (decline of 0.06 in 6 streams showing responses). Streamwater turbidity and conductivity did not show consistent responses during the eclipse. We suggest that decreased insolation directly reduced water temperature and concomitantly curtailed stream periphyton photosynthesis, leading to reduced dissolved O_2 production and increased dissolved CO_2 concentrations (lowering pH). Declines in dissolved O_2 and pH were greatest in 1st- and 2nd-order streams with high sun exposure, low gradients, and the widest arrays of aquatic vegetation (periphyton, filamentous algae, aquatic macrophytes, and emergent vegetation). Streams with morning shade from topography or tree-lined banks had responses that were smaller in magnitude. Stream basin area, discharge volume, and current velocity were not related to the magnitude of stream responses. Although the abiotic and biotic streamwater-quality responses to the eclipse were clear and measurable, the small magnitudes of the changes were well within the realm of diel variation and likely had minimal effect on the ecology of the stream ecosystem.

Key words: Algae, carbon dioxide, carbonic acid, dissolved oxygen, freshwater, lotic habitat, solar radiation, specific conductivity, water chemistry

Solar eclipses are relatively rare events, occurring somewhere on Earth 2.37 times per year, on average. Of these, 27% are total eclipses, 33% are annular eclipses, 35% are partial eclipses, and 5% are hybrid eclipses (NASA 2016). During annular solar eclipses, the moon covers 91.7 to 99.9% of the sun, compared with 100% during total eclipses (NASA 2016). Insolation reductions during an eclipse produce short-term, near-land-surface atmospheric dynamics, including air temperature reductions, relative humidity increases, changes in atmospheric ozone, reductions in wind speed, and changes in wind direction (Aplin et al. 2016, Clark 2016, Chernogor 2021, Nelli et al. 2021, Lazzús et al. 2022).

Ecological effects of solar eclipses include well-documented changes in behavior of terrestrial animals, including vertebrates and insects, as a result of reduced light levels simulating a sunset/dusk period followed by a sunrise/dawn period (Ritson et al. 2019, Hartstone-Rose et al. 2020). Similarly, in aquatic ecosystems, eclipse events have been shown to influence behaviors of plankton, invertebrates, and fish in marine and lentic freshwater settings (Backus et al. 1965, Skud 1967, Vecchione et al. 1986, Giroud and Balvay 1999, Adhikari et al. 2018). Only a single study has examined eclipse effects in a stream ecosystem (Suter and Williams 1977), and that study was limited to aquatic insect drift and recorded no substantial eclipse-related changes.

The primary drivers of stream and riverine ecosystem structure and functioning are solar inputs/thermal regimes, flow dynamics, and nutrients (Bernhardt et al. 2018, 2022). Stream primary productivity varies as a function of solar irradiance, shading from riparian vegetation, substrate type,

Email addresses: [4]Robert_Parmenter@partner.nps.gov, parmentr@unm.edu; [5]agrendys@usgs.gov; [6]David_Pittenger@nps.gov; [7]Greg.McCurdy@dri.edu

Received 1 December 2023; Accepted 24 April 2024; Published online 17 September 2024. Associate Editor, Janice Brahney.

Freshwater Science, volume 43, number 4, December 2024. https://doi.org/10.1086/732799

and disturbance regimes (Boston and Hill 1991, Hill et al. 2011, Heaston et al. 2018). Benthic periphyton, filamentous algae, and aquatic vascular plants all contribute O_2 to the streamwater column while taking up CO_2 during the photosynthetic process, and any environmental variable that affects light transmission and attenuation into streams (e.g., diel light cycles, vegetation shading, stream turbidity) will alter photosynthetic rates and influence streamwater quality (Julian et al. 2008, Law 2011, Atkinson and Cooper 2016, Jia et al. 2020, Kirk et al. 2021, Savoy et al. 2021, Savoy and Harvey 2021). Solar eclipses influence solar irradiance and, therefore, should have quantifiable effects on streamwater quality via potential temperature declines and changes in dissolved O_2 and pH from reductions of instream photosynthesis.

In this study, we addressed the impact of the 14 October 2023 annular solar eclipse on a hierarchical series of montane streams in New Mexico, USA. Specifically, we explored how streamwater-quality variables respond to decreased insolation during an annular solar eclipse, and we assessed if those responses are mediated by stream physical conditions such as discharge rates, current velocities, and basin area. We evaluated stream responses under 2 potential scenarios: 1) stream responses would be dominated by abiotic, physical processes; and 2) stream responses would be dominated by biological and chemical processes. We predicted that if stream responses were driven primarily by abiotic processes, then 1) streamwater temperatures would drop with reductions in insolation, 2) dissolved O_2 would increase as a function of water temperature declines, and 3) pH would remain unchanged in its normal diel cycle. In contrast, we predicted that if stream responses to the eclipse were driven by biological and chemical processes, then declines in light-driven photosynthetic processes by aquatic algae and macrophytes would result in 1) short-term decreases in streamwater dissolved O_2 concentrations and 2) concomitant increases in dissolved CO_2 levels, shifting the chemical equilibrium of dissolved CO_2 towards increased carbonic acid concentration and leading to lower pH levels. However, the potential magnitude and duration of these changes under either scenario were unknown.

METHODS

We utilized a network of existing weather stations in the study region to document near-ground-level atmospheric dynamics before, during, and after the annular solar eclipse on 14 October 2023, and we expanded a network of long-term streamwater-quality instruments to capture eclipse-related dynamics over a range of 1st- to 4th-order streams. At 7 stream reaches, we collected data on streamwater temperature, discharge, flow velocity, dissolved O_2, pH, conductivity, and turbidity. We assessed diel patterns of atmospheric and streamwater-quality variables to determine whether they deviated from normal during the eclipse period. Finally, we fit linear and nonlinear models to evaluate whether streamwater-quality responses to the eclipse varied with stream-basin size or flow variables.

Study site

The Jemez River drains the central and southwestern portions of the Jemez Mountains in northern New Mexico, USA (Fig. 1). The watershed includes the United States National Park Service's Valles Caldera National Preserve (VCNP) and the United States Forest Service's Santa Fe National Forest (SFNF). The terrain is characterized by volcanic formations created by a series of eruptions over the last 1.23 million y (Goff 2009). VCNP comprises the upper watershed with multiple 1st- and 2nd-order streams flowing through the caldera wall to the southwest, creating the 3rd-order upper Jemez River at the confluence of the East Fork Jemez River and the Rio San Antonio (Figs 1, 2A–G). The 3rd-order Rio Guadalupe and its tributaries drain the western slope of the caldera and join the Jemez River near Cañon, New Mexico, forming the 4th-order lower Jemez River. Vegetation in the Jemez Mountains consists of spruce-fir and mixed-conifer forests at the highest elevations (3430 m), grading downward through pine forests and piñon-juniper woodlands. Open grasslands (valles) are interspersed among the forested volcanic peaks.

In total, we deployed instruments in 7 streams, including the two 1st-order streams, two 2nd-order streams, two 3rd-order streams, and one 4th-order stream (Table 1). The 1st- and 2nd-order streams were part of an existing stream monitoring network operating on VCNP since 2005. The 3rd- and 4th-order stream sites were added for this study.

The two 1st-order streams were both in upland meadow habitats but were different in several aspects. Indios Creek was the smallest stream (Fig. 2A), with the lowest discharge but with a higher gradient and twice the current velocity of the 1st-order headwater stream of the Rio San Antonio (Fig. 2B) in the Valle Toledo (Table 1; Goodman 2003, Nelson and Manickam 2007). In addition, the water sources of Indios Creek were a series of higher-elevation montane canyon springs (with colder temperatures; diel range during our study of 0.0–9.0°C), whereas the Rio San Antonio's water was derived from upwelling groundwater under Artesian pressure (with higher temperatures; diel range of 8.5–14.5°C) within the Valle Toledo (Liu et al. 2008). There were comparable diel dissolved O_2 fluctuations in both streams (~7–10 mg/L), but there was little change in pH in Indios Creek (~7.5) compared with the Rio San Antonio (pH range of 7.4–8.7). Finally, Indios Creek had a smaller stream width and width-to-depth ratio than Rio San Antonio (Table 1), which, coupled with a steeply incised channel and extensive overhanging sedges (*Carex* spp.), shaded much of Indios Creek from direct morning sunlight (Fig. 2A).

The two 2nd-order streams, the Rio San Antonio at the western boundary of VCNP (Fig. 2C) and the East Fork Jemez River in the Valle Grande of VCNP (Fig. 2D), were

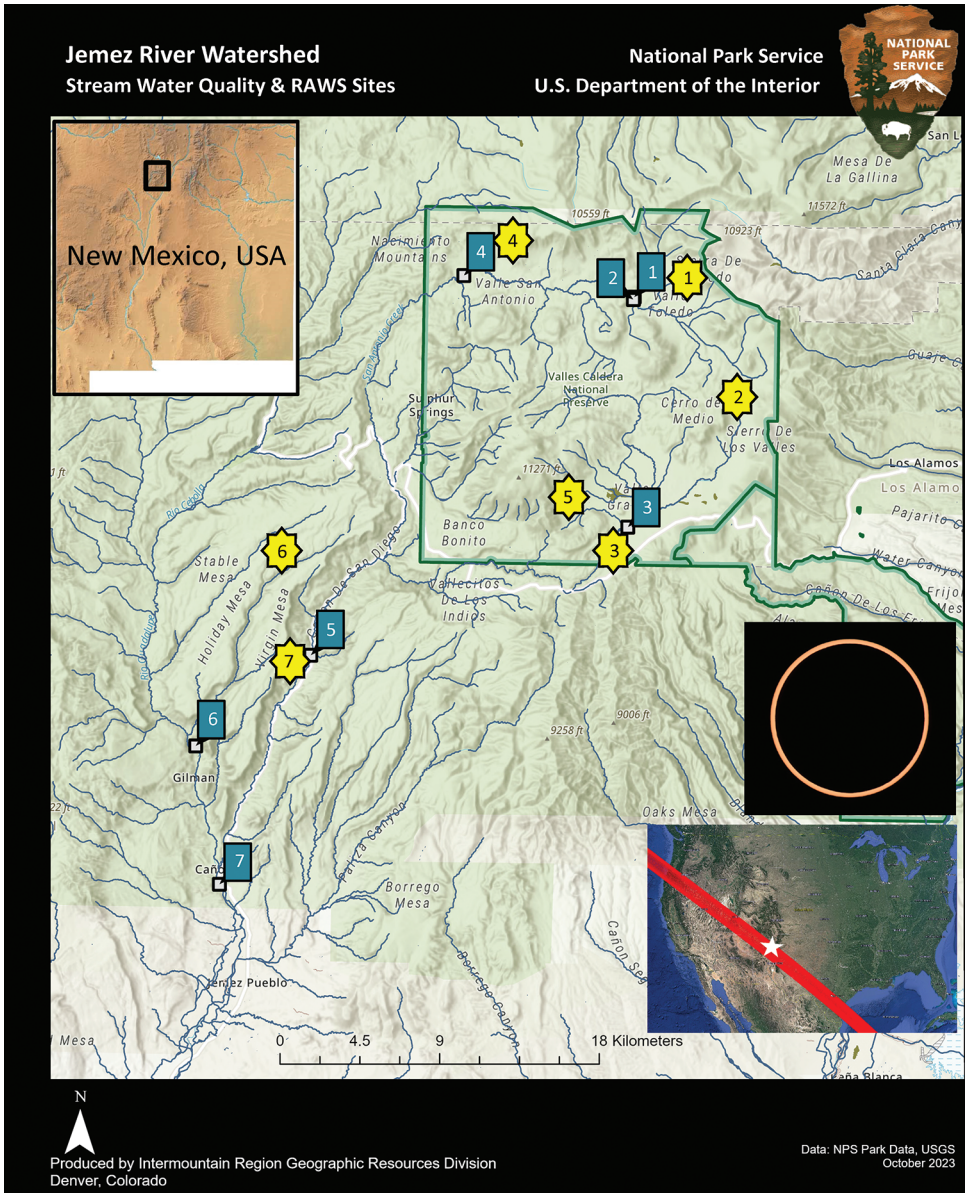

Figure 1. Map of stream sampling locations in the Jemez River watershed, New Mexico, USA. Upper left inset: Location of Jemez Mountains in New Mexico. Center: Study area with perennial stream sampling sites (blue boxes) and Remote Automatic Weather Stations (yellow stars). See Table 1 for site information. Bottom right inset: Eclipse track (red band) across western North America with location of Jemez Mountains (white star)—image courtesy of NASA. Photo above inset: Annular solar eclipse taken in Albuquerque, New Mexico, 14 October 2023, 10:37 h (Mountain Daylight Savings Time)—photo by Fraser and Cathy Goff, with permission. NPS = National Park Service, USGS = United States Geological Survey.

both in open, sunny meadow habitats (i.e., valles) with similar discharge, stream widths, gradients, and riffle-to-pool ratios (Table 1; Simino 2002, Goodman 2003). Both streams supported large amounts of periphyton, filamentous algae, aquatic vascular plants (e.g., *Elodea canadensis*, *Ranunculus aquatilis*), and emergent streambank sedges, associated with high instream gross primary production (Summers et al. 2020) and rapid nutrient uptake rates (Van Horn et al. 2012). Both streams shared similar water-quality values and diel cycles, except that the East Fork Jemez River had a higher level of turbidity than the Rio San Antonio (Table 1).

The two 3rd-order streams, the upper Jemez River (Fig. 2E) and the Rio Guadalupe (Fig. 2F), were similar in their topographic locations (bottoms of large canyons). They both had tree-lined, shaded banks dominated by Rio Grande cottonwood (*Populus deltoides* ssp. *wislizeni*) and willows (*Salix* spp.), which, in mid-October, still retained their leaves. These streams shared comparable stream widths, current

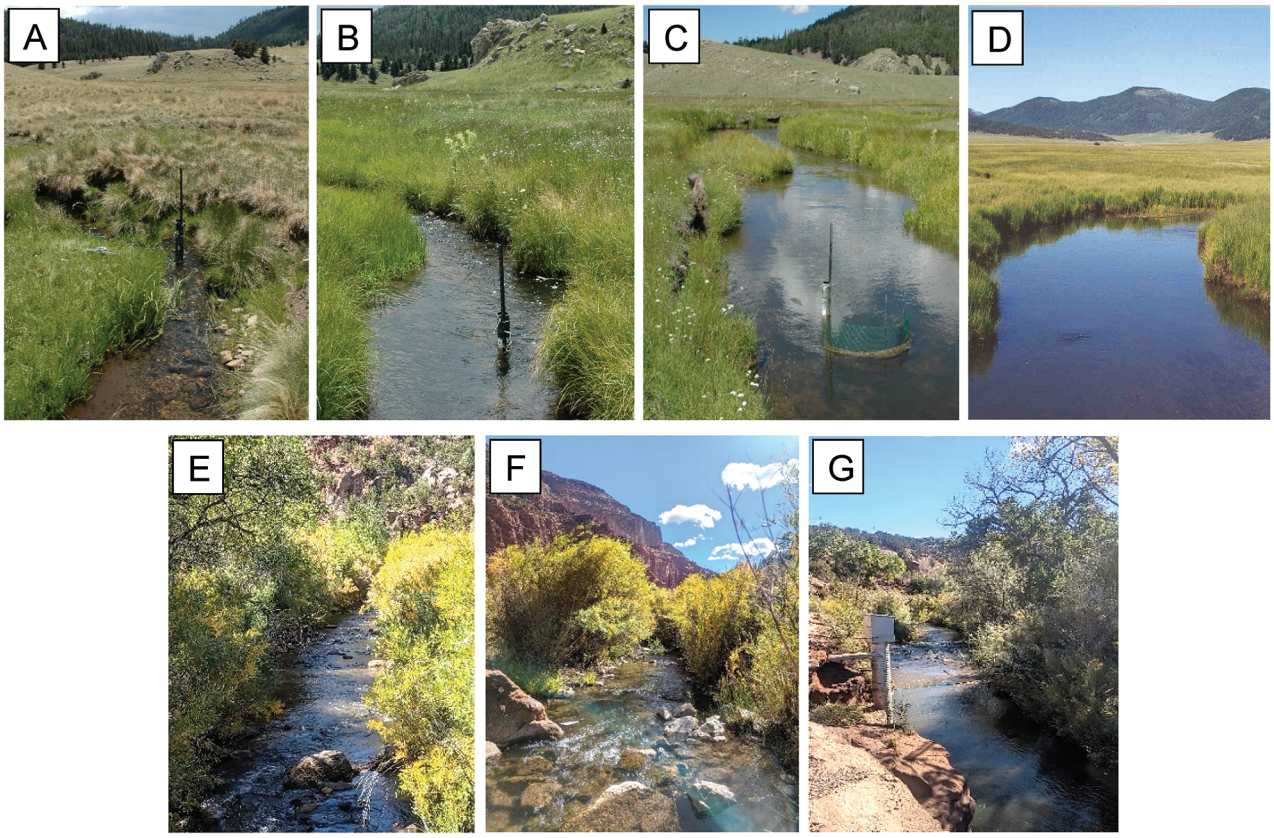

Figure 2. Photos of perennial stream study sites in the Jemez River watershed, New Mexico, USA. Indios Creek: 1st-order stream (A); Rio San Antonio, Valle Toledo: 1st-order stream (B); Rio San Antonio West: 2nd-order stream (C); East Fork Jemez River, Valle Grande: 2nd-order stream (D); Jemez River in Jemez Springs: 3rd-order stream (E); Rio Guadalupe: 3rd-order stream (F); Jemez River at United States Geological Survey Jemez gauge: 4th-order stream (G). Photos: National Park Service staff.

velocities, and riffle-to-pool ratios (Anderson et al. 2006, Galindo 2010), along with similar water-quality values and diel cycles (Table 1). However, the Jemez River had nearly twice the discharge as the Rio Guadalupe, and the Rio Guadalupe had a much steeper gradient upstream from the study site than the Jemez River (Table 1).

The 4th-order stream, the Jemez River below the confluence of the Rio Guadalupe and the upper Jemez River (Fig. 2G), had the greatest discharge and the fastest current (Table 1). The Jemez River also had the highest water temperature, pH, and conductivity and the 2nd-highest turbidity. Like the 2 upstream sites, this reach supported tree-lined riparian zones that shaded much of the stream during morning periods.

Meteorological data

VCNP and the Western Regional Climate Center, Desert Research Institute, operate a network of Remote Automatic Weather Stations (RAWS) across the Jemez Mountains (Fig. 1). These stations record air temperature, relative humidity, total solar radiation, precipitation, and wind speed and direction every minute and report the data as 10-min interval averages. For the period of the eclipse, we used data from the 7 RAWS that were at similar elevations to the stream monitoring locations (Table 1, Fig. 1): Valle Toledo, Valle de los Posos, Hidden Valley, Valle Grande, Valle San Antonio, Cebollita Springs, and Jemez Springs (see https://wrcc.dri.edu/vallescaldera/).

Streamwater-quality data

The National Park Service conducts long-term monitoring of streamwater quality and discharge on 1st- and 2nd-order streams on VCNP (Fig. 1), and the United States Geological Survey (USGS) operates a stream gauge on the 4th-order Jemez River near Cañon (Jemez, New Mexico gauge #08324000). In anticipation of the annular solar eclipse, we expanded the water-quality monitoring network to include 3rd- and 4th-order stream sites in the lower reaches of the Jemez River basin.

To monitor streamwater quality during the eclipse, we used YSI multiparameter water-quality sonde instruments (model EXO$^{3™}$, Yellow Springs Instruments, Yellow Springs, Ohio) equipped with an EXO wiped conductivity and temperature sensor (measurement resolutions of 0.001 µS/cm [standardized to 25°C] and 0.001°C, respectively), an EXO optical dissolved O_2 smart sensor (resolution of 0.01 mg/L), an EXO unguarded pH smart sensor (resolution of 0.01 pH

Table 1. Study site characteristics, locations, and elevations of perennial streams and RAWS sites in the Jemez River watershed, New Mexico, USA. Stream and RAWS ID numbers refer to the map in Fig. 1. Data on discharge, current velocity, and water-quality variables were collected during the study period of 13 to 15 October 2023. Water-quality variables are reported as means over the 3-d period. Aquatic plant types are P = periphyton, FA = filamentous algae, AVP = aquatic vascular plants, and EM = emergent macrophytes. USGS = United States Geological Survey.

Stream characteristic	Indios Creek[a]	Rio San Antonio, Valle Toledo[b]	East Fork Jemez River, Valle Grande[c]	Rio San Antonio, West[b]	Jemez River at Jemez Springs[d]	Rio Guadalupe[e]	Jemez River at USGS gauge[d]
Stream ID#	1	2	3	4	5	6	7
Stream order	1st	1st	2nd	2nd	3rd	3rd	4th
Basin area (km^2)[f]	18	50	94	147	471	684	1217
Discharge (m^3/s)	0.0065	0.0578	0.0708	0.0937	0.2568	0.1314	0.3794
Current velocity (m/s)	0.2743	0.1372	0.0914	0.2134	0.1676	0.1737	0.3597
Reach length (km)[g]	3.48	1.93	5.95	19.31	2.33	0.80	11.23
Rosgen channel type	E5	E5	E6	E4	C2	A3	C3
Gradient (%)	1.80	0.05	0.05	0.30	1.60	6.10	1.00
Mean stream width (m)	0.91	2.08	4.48	4.05	6.48	8.54	5.80
Bankfull width:depth ratio	2:1	7:1	14:1	7:1	26:1	16:1	22:1
Riffle:pool (%)	71:29	95:05	94:06	97:03	88:12	81:19	90:10
Substrate: Riffle							
Sand (%)	47.1	36.4	59.0	40.3	17.9	9.2	33.6
Gravel (%)	46.4	36.4	41.0	44.4	13.6	17.5	18.5
Cobble (%)	6.4	22.7	0.0	14.7	27.1	28.3	35.0
Boulder–bedrock (%)	0.1	4.5	0.0	0.6	41.4	45.0	12.9
Substrate: Pool							
Sand (%)	53.3	85.7	67.0	76.5	43.1	11.7	43.5
Gravel (%)	40.6	10.0	33.0	21.0	10.8	18.3	15.9
Cobble (%)	5.9	4.3	0.0	2.0	19.2	28.3	29.6
Boulder–bedrock (%)	0.2	0.0	0.0	0.5	26.9	41.7	11.0
Aquatic plants	P, FA	P, FA, AVP, EM	P, FA, AVP, EM	P, FA, AVP, EM	P, FA, AVP	P, FA	P, FA
Water-quality variables							
Temperature (°C)	3.4	10.8	5.0	6.4	10.4	7.9	11.2
Dissolved O_2 (mg/L)	9.3	8.2	9.2	8.5	8.7	9.3	8.5
O_2 saturation (%)	93.6	100.5	97.2	92.7	98.2	101.0	100.9
pH	7.5	7.8	7.7	7.8	8.0	8.5	8.7
Specific conductivity (µS/cm)	79.1	78.8	84.4	107.5	785.8	263.5	849.3
Turbidity (FNU)	7.0	1.1	20.1	5.0	3.8	2.3	8.4
Sonde location							
Latitude (NAD83)	35.9638	35.9626	35.8470	35.9734	35.7793	35.7322	35.6621
Longitude (NAD83)	−106.4902	−106.4906	−106.4920	−106.5969	−106.6885	−106.7592	−106.743
Elevation (m)	2615	2612	2589	2554	1910	1830	1714
RAWS location	Valle Toledo	Valle de los Posos	Hidden Valley	Valle San Antonio	Valle Grande	Cebollita Springs	Jemez Springs
RAWS ID#	1	2	3	4	5	6	7
Latitude (NAD83)	35.9739	35.9158	35.8408	35.9806	35.8583	35.8311	35.7797
Longitude (NAD83)	−106.4647	−106.4228	−106.5006	−106.5708	−106.5211	−106.7208	−106.6890
Elevation (m)	2750	2738	2582	2598	2643	2496	1924

[a] Nelson and Manickam (2007)
[b] Goodman (2003)
[c] Simino (2002)
[d] Galindo (2010)
[e] Anderson et al. (2006)
[f] Area above sonde location
[g] Length of stream reach with sonde surveyed in the cited references

units), and an EXO turbidity smart sensor (with wiper, resolution of 0.01 NFU). We secured sondes vertically to steel T-posts in each stream's thalweg, with sensors positioned at depths of 15 to 30 cm. We calibrated sensors just prior to deployment. We set the sondes to record measurements every 5 min for 3 d, beginning at 00:00:00 Mountain Daylight Time (MDT) on 13 October 2023 and running through 00:00:00 MDT on 16 October 2023. This 3-d time period provided data for the day before the eclipse, the day of the eclipse, and the day following the eclipse.

In selecting stream study sites, we chose locations that were separated by distances of 9.5 to 51.9 km within the Jemez River watershed to ensure independence of measurements during the period of the eclipse. Based on measurements of stream current at the sites (Table 1), the travel times for water between sites ranged from 7.3 to 84.7 h. Given that the eclipse period was predicted to last just under 3 h (NASA 2016), instrument records would have been independent of neighboring upstream study sites.

Atmospheric and streamwater-quality responses to eclipse

We evaluated the data to determine if diel patterns of atmospheric and streamwater-quality variables deviated from normal increases/decreases during the period of the eclipse compared with the days prior to and after the eclipse. We compared the data values during the eclipse with the mean data values taken at the same time of day from the day before and the day after the eclipse. We then determined the magnitude of differences between the eclipse period and the mean of the pre- and post-eclipse periods at the same time periods. For meteorological data, the time of maximal deviation was 10 to 20 min after annularity (i.e., RAWS samples recorded at 10:50 and 11:00 h), whereas for stream data, maximal deviation coincided with annularity (with the 10:40-h sonde samples).

Given observed declines in streamwater temperatures, we calculated the expected (theoretical) changes in dissolved O_2 that would have followed the observed temperature changes during the eclipse. To do so we used the USGS program DOTABLES (version 3.6; USGS 2011; https://water.usgs.gov/water-resources/software/DOTABLES/) based on the models of Benson and Krause (1980, 1984). Model inputs included observed barometric pressure, streamwater temperature, specific conductivity, and dissolved O_2, which produced model outputs of potential maximum dissolved O_2 content (mg/L). We ran the program for 1) the mean values of pre- and post-eclipse days and 2) the eclipse period. We then compared the difference in the predicted changes with the observed changes recorded by the sondes to assess whether purely physical/abiotic processes were dominating stream responses to the eclipse or whether biotic/chemical processes were important.

Finally, we fit individual linear and nonlinear (exponential, logarithmic, hyperbolic, polynomial) regressions to test for relationships between the magnitude of eclipse responses of streamwater-quality variables (dependent variables) and stream discharge, current velocity, and basin size (independent variables) and used 2-tailed probabilities for determination of the strength of evidence for effects. We verified regression assumptions with the Shapiro and Wilk (1965) normality test for residuals, a runs test (Sokal and Rohlf 1969) for residual autocorrelation, and plots of fitted values vs residuals for homoscedasticity. We conducted statistical analyses with the software package Statistix 10 (Analytical Software, Tallahassee, Florida).

RESULTS

Eclipse data

Weather conditions during the days leading up to the eclipse and following the eclipse were cloudless and sunny because of a sustained high-pressure system over New Mexico. Barometric pressure increased only slightly (1100–1200 pa) over the 3 d of the study. The annular solar eclipse began over the study area on Saturday, 14 October 2023, at 09:13:14 MDT and ended at 12:08:59 MDT, lasting for 175.75 min. The annularity (maximum eclipse period) lasted for 3.13 min (10:35:14–10:38:22 MDT). The path width of the eclipse was 201 km. At maximum, the eclipse magnitude was 0.946 on the study site for the 3.13-min duration of the maximal eclipse period (see https://eclipse.gsfc.nasa.gov/SEdecade/SEdecade2021.html).

Atmospheric data

Maximal changes in weather variables often occurred 10 to 20 min after the eclipse annularity (maximal reduction in solar radiation). Maximal deviations in post-annularity values for temperature, humidity, and wind were recorded at 10:50 and 11:00 h. Based on the greatest deviation values averaged over the 7 RAWS stations, the eclipse resulted in a mean (±SE) reduction in solar radiation of 544 ± 8.9 W/m^2 (92.0 ± 0.1%), a decline in air temperatures of 6.7 ± 0.9°C (range of 4.0–9.1°C), and an increase in relative humidity of 16.2 ± 3.1% (range of 7.8–24.8%; Table 2). Mean wind speed during the eclipse dropped 1.2 ± 0.3 m/s (59.1%), and the maximum wind gust speed declined 2.2 ± 0.5 m/s (55.5%), but wind conditions continued during the eclipse with a mean wind speed of 0.82 ± 0.18 m/s and wind gusts of 1.53 ± 0.28 m/s. (See Fig. 3A–D for example results from Valle San Antonio RAWS and Figs S1–S6A–D for the other RAWS sites.)

Stream data

Prior to the eclipse, the study area had received no precipitation for 12 d, and all of the streams were at base flow. During the eclipse, the sonde instruments recorded distinct

Table 2. Summary of changes in meteorological variables at Remote Automatic Weather Stations (RAWS) in the Jemez Mountains, New Mexico, USA, during the 14 October 2023 annular solar eclipse. RAWS ID #s refer to the map in Fig. 1. Values are the differences between measurements of maximal deviations during the eclipse and the mean of the measurements collected at the same times on the day before and the day after the eclipse.

RAWS station	ID#	Δ solar radiation (W/m^2)	Δ mean air temperature (°C)	Δ relative humidity (%)	Δ mean wind speed (m/s)	Δ maximum wind gust speed (m/s)
Valle Toledo	1	−527	−4.6	7.8	−0.90	−1.73
Valle de los Posos	2	−571	−6.8	15.3	−1.11	−1.86
Hidden Valley	3	−575	−8.6	23.7	−0.15	−0.54
Valle San Antonio	4	−534	−9.1	22.5	−2.35	−3.73
Valle Grande	5	−552	−8.9	24.8	−1.83	−3.60
Cebollita Springs	6	−523	−4.0	11.4	−1.10	−2.26
Jemez Springs	7	−527	−4.6	7.8	−0.90	−1.73

changes in the diel cycles of streamwater-quality variables in the study streams (Table 3). At the time of eclipse annularity (during the sonde sample for 10:35–10:40 h), stream temperatures in all 7 stream sites cooled by a mean of 0.67 ± 0.09°C (range of 0.46–1.05°C; Fig. 4A–G) and then resumed warming with the waning of the eclipse. Unlike atmospheric variables, streamwater-quality variables' deviations did not display a time lag after the maximum extent of the eclipse but coincided with the time of annularity. Streamwater maximum diel temperatures did not recover completely on the day of the eclipse, being on average 0.76°C cooler (Table 3), but completely recovered on the following day (Fig. 4A–G).

The other streamwater-quality parameters varied in their responses to the eclipse. In 5 of the 7 streams, dissolved O_2 declined by an average of 0.22 ± 0.12 mg/L (range of 0.04–0.62 mg/L), with similar declines in dissolved O_2 % saturation (Fig. S7A–G), but recovered later in the day (Fig. 4A–G). The 2 streams that did not show a dissolved O_2 decline

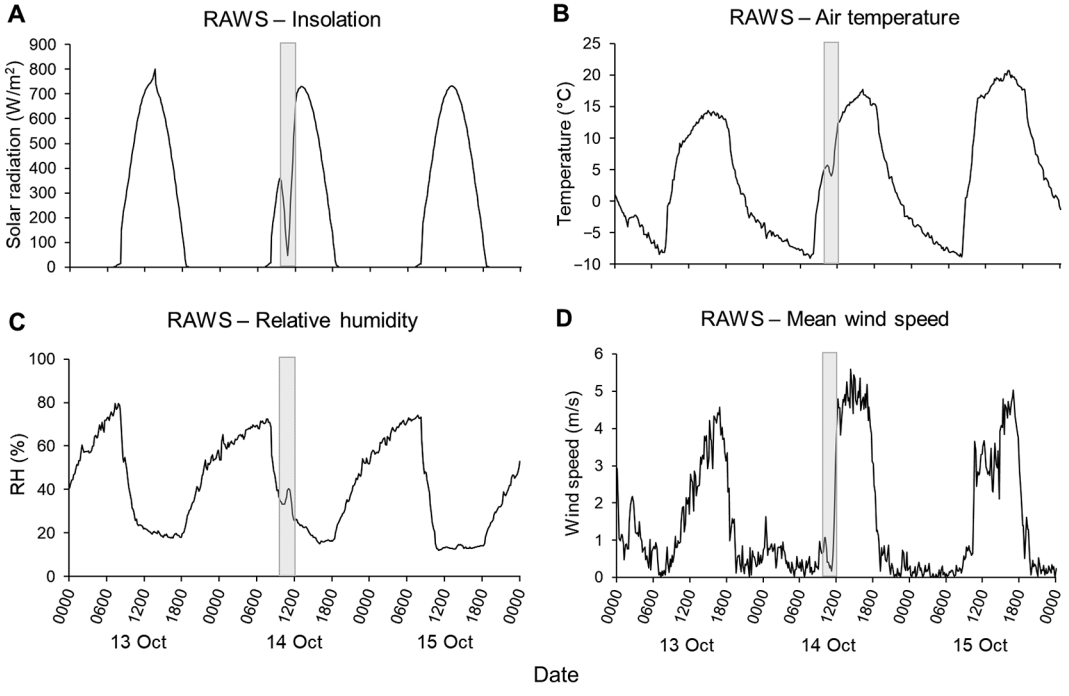

Figure 3. Valle San Antonio Remote Automatic Weather Station (RAWS) data during study period of annular solar eclipse (13–15 Oct 2023) on Valles Caldera National Preserve, New Mexico, USA. The shaded rectangle indicates the period of eclipse. Total solar radiation (A), air temperature (B), relative humidity (RH) (C), mean wind speed (D). (See Figs. S1–S6 for data from the other RAWS study sites.) Data from https://wrcc.dri.edu/vallescaldera/.

Table 3. Summary of changes in streamwater-quality variables in the Jemez River watershed, New Mexico, USA, during the 14 October 2023 annular solar eclipse. Stream ID #s refer to the map in Fig. 1. Values are the differences between measurements at the time of annularity (maximal eclipse at 1040 h Mountain Daylight Time) and the mean of the measurements collected at the same time on the day before and the day after the eclipse. USGS = United States Geological Survey.

Water-quality variable	Indios Creek	Rio San Antonio, Valle Toledo	East Fork Jemez River, Valle Grande	Rio San Antonio, West	Jemez River at Jemez Springs	Rio Guadalupe	Jemez River at USGS gauge
Stream ID#	1	2	3	4	5	6	7
Δ water temperature (°C)	−0.46	−0.66	−0.63	−0.90	−0.49	−1.05	−0.53
Δ maximum diel water temperature (°C)	−0.83	−0.44	−0.75	−1.22	−0.35	−0.92	−0.79
Δ range in water temperature (°C)	−0.84	−0.54	−0.91	−1.59	−0.27	−0.47	−0.62
Δ dissolved O_2 (mg/L)	0.01	−0.63	−0.26	−0.13	−0.04	−0.05	0.00
Δ pH	−0.01	−0.22	−0.04	−0.06	−0.01	−0.04	0.00

were the Indios Creek (1st-order stream with the smallest discharge; Fig. 4A) and the Jemez River at the USGS Jemez gauge (4th-order stream with the largest discharge; Fig. 4G). There was a mean decrease in pH of 0.06 ± 0.04 (range of 0.01–0.22) in 6 of the 7 streams (all except the 4th-order Jemez River at the USGS Jemez gauge, in which pH did not respond), and these streams' pH recovered to their normal dynamic pattern later in the day (Fig. 4G). Streamwater turbidity (Fig. S8A–G) did not respond consistently to the eclipse, and only 2 streams had small-magnitude increases in conductivity (Rio San Antonio at Valle Toledo and the Rio Guadalupe; Fig. S9B, F).

The predicted change in streamwater dissolved O_2, given the observed declines in temperature, indicated that dissolved O_2 should have increased by an average of 0.18 ± 0.04 mg/L (Table 4). However, dissolved O_2 actually declined, leading to an overall effective change of –0.34 ± 0.18 mg/L on average across all 7 stream sites (Table 4).

Linear and non-linear regression analyses of water-quality variables (temperature, dissolved O_2, and pH) and stream

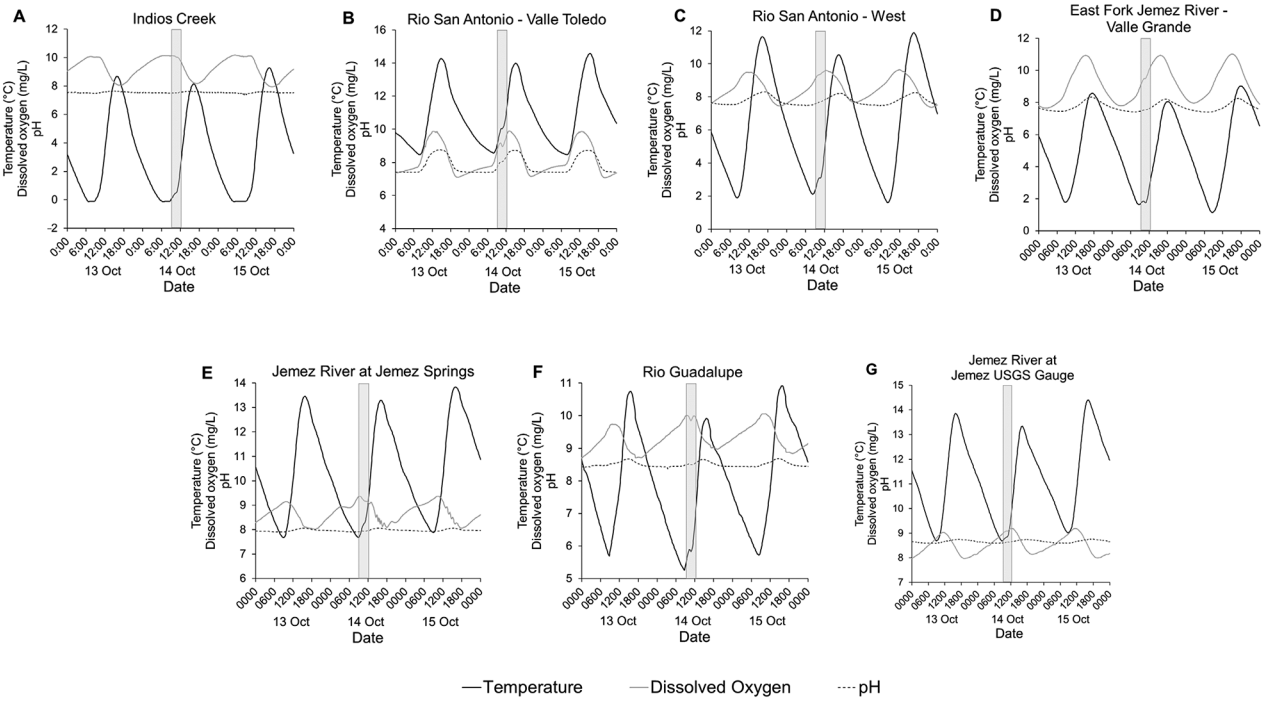

Figure 4. Changes in streamwater quality for temperature, dissolved O_2, and pH during the annular solar eclipse study period (13–15 October 2023) in the Jemez Mountains, New Mexico, USA. The shaded rectangle indicates the period of eclipse. 1st-order streams (A, B), 2nd-order streams (C, D), 3rd-order streams (E, F), 4th-order stream (G). See Fig. 1 for stream locations. USGS = United States Geological Survey.

Table 4. Calculated site-specific increases in stream dissolved O_2 (DO) with observed stream temperature decreases at the stream study sites in the Jemez River watershed, New Mexico, USA, during the 14 October 2023 annular solar eclipse. Stream ID #s refer to the map in Fig. 1. USGS = United States Geological Survey.

Stream study site	Site ID#	Observed Δ streamwater temperature (°C)	Theoretical Δ DO (mg/L)	Observed Δ DO (mg/L)	Difference in Δ DO (mg/L) attributed to biological processes
Indios Creek	1	−0.46	0.17	0.01	−0.16
Rio San Antonio (Toledo)	2	−0.66	0.15	−0.63	−0.78
East Fork Jemez River, Valle Grande	3	−0.62	0.20	−0.26	−0.47
Rio San Antonio (West)	4	−0.90	0.24	−0.13	−0.37
Jemez River in Jemez Springs	5	−0.49	0.12	−0.04	−0.17
Rio Guadalupe	6	−1.05	0.26	−0.04	−0.31
Jemez River at USGS Jemez gauge	7	−0.53	0.12	0.00	−0.12

discharge, current velocity, and watershed basin area did not identify any meaningful relationships (r^2 values of 0.002–0.389 [$n = 7$], p-values ranged from 0.13–0.92).

DISCUSSION

The annular solar eclipse in the Jemez Mountains produced substantial reductions (92%) in solar radiation, which led to near-ground-level decreases in air temperature and wind speeds and increases in relative humidity (Figs 3A–G, S1–S6A–G). Our recorded values for atmospheric changes during the eclipse were comparable with previous studies. Aplin et al. (2016) reviewed ~120 previous reports on eclipse effects on near-ground weather conditions and found consistent reductions in air temperature (with a maximum decline of ~7°C). Our RAWS sites recorded an average decline of 6.7°C. Recent reports on relative humidity changes indicate increases of 3 to 19% during an eclipse (Brinley Buckley et al. 2018, Lazzús et al. 2022 and references therein), and we found an increase in relative humidity of 16%. Wind speed reductions during eclipses of ~1 to 2 m/s have been reported (Lazzús et al. 2022 and references therein), and, accordingly, our study sites had a reduction in wind speed of 1.2 m/s. As with previous studies, we observed a time lag of 10 to 20 min past the time of annularity until recording maximum deviations in atmospheric temperature and humidity. Aplin et al. (2016 and references therein) reviewed eclipse studies reporting 6- to 30-min time lags for temperature, as well as a 28-min mean time lag for humidity. The authors suggested that the thermal inertia of the Earth's surface layer, in concert with solar irradiance levels during the latter part of the eclipse (4th contact period), may be responsible for the time lags.

As recorded by the sondes, the eclipse produced distinct, small-magnitude, short-term reductions in streamwater temperature in all of the streams, as well as small, short-term reductions in dissolved O_2 and pH in most of the streams (Fig. 4A–G). We interpret the lower streamwater temperatures as consistent with the decrease in insolation, with water temperature directly influenced by reduced infrared radiation. This observation supports the role of abiotic, physical processes driving the streamwater temperature response to the eclipse. However, we predicted that if abiotic processes were the sole process, then dissolved O_2 would increase with a lower water temperature and pH would be unaffected. Instead, we observed a decrease in dissolved O_2 and pH. We interpret these changes to be a result of decreased photosynthetic activity by stream algae/periphyton and macrophytes, which would have curtailed dissolved O_2 production and dissolved CO_2 uptake. With a 92% reduction in insolation, photosynthesis would have been nearly terminated, greatly reducing dissolved O_2 production and restricting the uptake of CO_2. The resulting increase in dissolved CO_2 from ongoing ecosystem respiration would have favored the equilibrium concentration of carbonic acid ($H_2O + CO_2 \rightleftharpoons HCO_3^- + H^+$), thereby decreasing pH. The observed declines in dissolved O_2 were large enough to overcome the predicted abiotic increases in dissolved O_2 with decreasing water temperatures (Table 4), supporting the conclusion that biotic/chemical processes were the main drivers of the streams' dissolved O_2 and pH responses to the eclipse.

We found no distinguishable patterns of eclipse responses in streamwater temperature, dissolved O_2, or pH across the range of stream orders (including basin size, discharge, and current velocity), although the 2 streams with the smallest temperature changes and without changes in dissolved O_2 and pH were the smallest stream (Indios Creek) and the largest river (Jemez River at the USGS Jemez gauge). The 1st-order Indios Creek is characterized by an incised channel and overhanging sedges that provided considerable shade from the morning sun across the stream's surface (Fig. 2A), which presumably lessened the net effect of reduced insolation; however, the reduction in photosynthesis activity by the Indios Creek periphyton community was sufficiently large that it cancelled out the theoretical increase in dissolved O_2 from lower water temperatures

(Table 4), resulting in a no-change sonde record. In contrast, the 4th-order Jemez River (Fig. 2G) had such a large water volume (discharge and current velocity), high turbidity, and shaded, tree-lined riparian banks that the decreased insolation constituted a very small change in energy input relative to the volume of water in the river, thereby potentially masking any discernible response by streamwater-quality variables. However, as with Indios Creek, the presumed lower periphyton photosynthesis within this reach compensated for any temperature-induced increase in dissolved O_2, producing a no-change sonde record.

We observed the largest stream responses to the eclipse in the 2 Rio San Antonio sites and East Fork Jemez River site. These reaches had the greatest array of aquatic plants (periphyton, filamentous algae, aquatic vascular plants, and emergent macrophytes), as well as the lowest gradient, slowest current (Table 1), and greatest solar exposure (Fig. 2B–D). Although their streamwater temperatures declined by a similar magnitude as the other streams, these reaches had the greatest decreases in dissolved O_2 and pH (Table 3), indicating that photosynthesis had a greater effect than abiotic dynamics on streamwater chemistry (Table 4). The higher-order streams (Rio Guadalupe and the Jemez River sites), which supported a smaller array of aquatic algae and vascular plants and which had shady, tree-lined banks (Fig. 2E–G), had smaller magnitude declines in dissolved O_2 and pH (Table 3) but still exceeded the predicted temperature-related increase in dissolved O_2 (Table 4). The higher photosynthetic response of the shallow, slow-moving, unshaded streams compared with the tree-shaded riverine reaches is consistent with studies comparing ecosystem primary production across a range of streams and rivers (Julian et al. 2008, Kirk et al. 2021, Savoy and Harvey 2021, Bernhardt et al. 2022).

We were unable to find any published reports of eclipse effects on streamwater quality, but a small number of studies have addressed eclipse effects on lentic aquatic ecosystems. These studies found similar water-quality responses, with declines in water temperature, dissolved O_2, and pH. During the 1980 total eclipse over the Nagarjunasagar Reservoir, India, Pathak and Sugunan (1980) found a 4°C drop in air temperature and a 1.5°C drop in water temperature. In addition, dissolved O_2 declined 0.72 mg/L, pH declined by 0.2 units, and bicarbonate increased from 90.24 to 98.88 mg/L; however, no substantial response by plankton to decreased sunlight was observed (Pathak and Sugunan 1980). Adhikari et al. (2018) observed changes in water quality during a total eclipse in an oxbow lake in India and found lower dissolved O_2 (decrease of 0.4 mg/L), increased community respiration, and a lower range of pH values during the eclipse. Water temperature did not respond to the eclipse, but plankton densities increased near the surface during the maximal darkness of the eclipse. Vecchione et al. (1986) observed increases in chlorophyll *a* in a shallow Louisiana, USA, estuary during an eclipse and proposed that microflagellates had migrated upwards in the water column during the reduced light period. Similarly, Giroud and Balvay (1999) recorded increased upward movement of zooplankton during the 1999 eclipse over Lake Geneva, Switzerland. Comparable eclipse responses for vertical migratory behavior of oceanic plankton (including bioluminescence behavior) were reported by Backus et al. (1965) and Skud (1967).

The ecological impact of the solar annular eclipse in our study was likely minimal because the entire period of change was very short (<3 h), and the changes in stream temperatures, dissolved O_2, and pH were of small magnitude (Table 3, Fig. 4A–G). The reductions in temperature during the early part of the day appeared to have delayed stream warming and reduced the maximum temperature for the day by 0.76°C (Table 3, Fig. 4A–G) compared with the day before, but stream temperatures recovered the following day. Dissolved O_2 and pH appeared to have recovered almost immediately, with values returning to pre- and post-eclipse-day levels later the same day (Fig. 4A–G). The magnitude of these changes in water-quality values were equivalent to similar temporal diel changes during dusk and dawn. Similarly, the eclipse effects we observed were comparable with those of a storm cloud during a summer monsoon in VCNP. For example, solar radiation values at our RAWS sites typically decline by ~80% during thunderstorms, compared with the eclipse reduction of 92% (Fig. 3A; data from https://wrcc.dri.edu/). Hence, although the annular solar eclipse resulted in distinct, observable effects on streamwater quality, the small magnitudes of these effects were within normal diel fluctuations in the study streams. Future solar eclipse events will undoubtedly provide comparable opportunities to examine streamwater-quality responses in lotic environments across other ecosystems, during varying times of day, and in different seasons.

ACKNOWLEDGEMENTS

Author contributions: RRP conceived the study, and RRP, ARG, and DWP planned and implemented the instrument recording. GDM operated the RAWS network and provided the meteorological data. All authors synthesized/analyzed the data, wrote/edited the manuscript, and provided final approval for publication.

We thank the National Park Service for providing the funding support for this project. The United States Geological Survey (USGS) provided the discharge data for the Jemez River at the Jemez gauge, and the Desert Research Institute (DRI) provided the weather data through the network of Remote Automatic Weather Stations (RAWS) in the Jemez Mountains. The National Aeronautics and Space Administration (NASA) provided the eclipse track map in Fig. 1, and the eclipse data were calculated by Fred Espenak and Alex Young, NASA Goddard Space Flight Center. Drs Fraser and Cathy Goff provided the eclipse photo in Fig. 1. We thank Tyler Obermeit for his assistance with the field work. We also thank 2 anonymous reviewers for their contributions, which improved our manuscript.

All study data are available at: https://irma.nps.gov/DataStore/Reference/Profile/2302681

LITERATURE CITED

Adhikari, S., A. R. Goswami, U. S. Roy, A. Aich, K. Datta, and S. K. Mukhopadhyay. 2018. Effect of a total solar eclipse on the surface crowding of zooplankton in a freshwater lake ecosystem. Limnology 19:253–270.

Anderson, T., D. Hoffman, and C. Dentino. 2006. Rio Guadalupe stream inventory report. Santa Fe National Forest, United States Department of Agriculture Forest Service, Santa Fe, New Mexico. (Available from: https://www.fs.usda.gov/detail/santafe/landmanagement/resourcemanagement/?cid=fsbdev7_021021)

Aplin, K. L., C. J. Scott, and S. L. Gray. 2016. Atmospheric changes from solar eclipses. Philosophical Transactions of the Royal Society A: Mathematical, Physical and Engineering Sciences 374:20150217.

Atkinson, C. L., and J. T. Cooper. 2016. Benthic algal community composition across a watershed: Coupling processes between land and water. Aquatic Ecology 50:315–326.

Backus, R. H., R. C. Clark Jr, and A. S. Wing. 1965. Behaviour of certain marine organisms during the solar eclipse of July 20, 1963. Nature 205:989–991.

Benson, B. B., and D. Krause Jr. 1980. The concentration and isotopic fractionation of gases dissolved in freshwater in equilibrium with the atmosphere. 1. Oxygen. Limnology and Oceanography 25:662–671.

Benson, B. B., and D. Krause Jr. 1984. The concentration and isotopic fractionation of oxygen dissolved in freshwater and seawater in equilibrium with the atmosphere. Limnology and Oceanography 29:620–632.

Bernhardt, E. S., J. B. Heffernan, N. B. Grimm, E. H. Stanley, J. W. Harvery, M. Arroita, A. P. Appling, M. J. Cohen, W. H. McDowell, R. O. Hall Jr, J. S. Read, B. J. Roberts, E. G. Stets, and C. B. Yackulic. 2018. The metabolic regimes of flowing waters. Limnology and Oceanography 63:S99–S118.

Bernhardt, E. S., P. Savoy, M. J. Vlah, A. P. Appling, L. E. Koenig, R. O. Hall Jr, M. Arroita, J. R. Blaszczak, A. M. Carter, M. Cohen, J. W. Harvey, J. B. Heffernan, A. M. Helton, J. D. Hosen, L. Kirk, W. H. McDowell, E. H. Stanley, C. B. Yackulic, and N. B. Grimm. 2022. Light and flow regimes regulate the metabolism of rivers. Proceedings of the National Academy of Sciences 119:e2121976119.

Boston, H. L., and W. R. Hill. 1991. Photosynthesis–light relations of stream periphyton communities. Limnology and Oceanography 36:644–656.

Brinley Buckley, E. M., A. J. Caven, B. L. Gottesman, M. J. Harner, B. C. Pijanowski, and M. L. Forsberg. 2018. Assessing biological and environmental effects of a total solar eclipse with passive multimodal technologies. Ecological Indicators 95:353–369.

Chernogor, L. F. 2021. Thermal effect in surface atmosphere of the solar eclipse on June 10, 2021. Kinematics and Physics of Celestial Bodies 37:293–299.

Clark, P. A. 2016 Numerical simulations of the impact of the 20 March 2015 eclipse on UK weather. Philosophical Transactions of the Royal Society A: Mathematical, Physical and Engineering Sciences 374:20150218.

Galindo, R. 2010. Jemez River stream inventory report. Santa Fe National Forest, United States Department of Agriculture Forest Service, Santa Fe, New Mexico. (Available from: https://www.fs.usda.gov/detail/santafe/landmanagement/resourcemanagement/?cid=fsbdev7_021021)

Giroud, C., and G. Balvay. 1999. The solar eclipse and the migration of some planktonic crustacea in Lake Geneva. Archives des Sciences 52:199–208.

Goff, F. 2009. Valles Caldera: A geologic history. University of New Mexico Press, Albuquerque, New Mexico.

Goodman, D. 2003. San Antonio Creek stream inventory report. Santa Fe National Forest, United States Department of Agriculture Forest Service, Santa Fe, New Mexico. (Available from: https://www.fs.usda.gov/detail/santafe/landmanagement/resourcemanagement/?cid=fsbdev7_021021)

Hartstone-Rose, A., E. Dickinson, L. M. Paciulli, A. R. Deutsch, L. Tran, G. Jones, and K. C. Leonard. 2020. Total eclipse of the zoo: Animal behavior during a total solar eclipse. Animals 10:587.

Heaston, E. D., M. J. Kaylor, and D. R. Warren. 2018. Aquatic food web response to patchy shading along forested headwater streams. Canadian Journal of Fisheries and Aquatic Sciences 75:2211–2220.

Hill, W. R., B. J. Roberts, S. N. Francoeur, and S. E. Fanta. 2011. Resource synergy in stream periphyton communities. Journal of Ecology 99:454–463.

Jia, J., Y. Gao, F. Zhou, K. Shi, P. J. Johnes, J. A. J. Dungait, M. Ma, and Y. Lu. 2020. Identifying the main drivers of change of phytoplankton community structure and gross primary productivity in a river-lake system. Journal of Hydrology 583:124633.

Julian, J. P., M. W. Doyle, S. M. Powers, E. H. Stanley, and J. A. Riggsbee. 2008. Optical water quality in rivers. Water Resources Research 44:W10411.

Kirk, L., R. T. Hensley, P. Savoy, J. B. Heffernan, and M. J. Cohen. 2021. Estimating benthic light regimes improves predictions of primary production and constrains light-use efficiency in streams and rivers. Ecosystems 24:825–839.

Law, R. 2011. A review of the function and uses of, and factors affecting, stream phytobenthos. Freshwater Reviews 4:135–166.

Lazzús, J. A., P. Vega-Jorquera, R. Pacheco, L. Tamblay, M. Martínez-Ledesma, E. M. Ovalle, E. Carrasco, M. Bravo, C. U. Villalobos, I. Salfate, L. Palma-Chilla, and A. J. Foppiano. 2022. Changes in meteorological parameters during the total solar eclipse of 2 July 2019 in La Serena, Chile. Annals of Geophysics 65:PA531.

Liu, F., R. Parmenter, P. D. Brooks, M. H. Conklin, and R. C. Bales. 2008. Seasonal and interannual variation of streamflow pathways and biogeochemical implications in semi-arid, forested catchments in Valles Caldera, New Mexico. Ecohydrology 1: 239–252.

NASA [National Atmospheric and Space Administration]. 2016. Solar eclipse website. (Available from: https://eclipse.gsfc.nasa.gov/solar.html, Accessed October 2023)

Nelli, N. R., M. Temimi, R. Fonseca, D. Francis, O. Nesterov, R. Abida, M. Weston, and A. Kumar. 2021. Anatomy of the annular solar eclipse of 26 December 2019 and its impact on land–atmosphere interactions over an arid region. Geoscience and Remote Sensing Letters 18:1312–1316.

Nelson, J, and Z. Manickam. 2007. Stream habitat survey report: Rito de los Indios. Santa Fe National Forest, United States Department of Agriculture Forest Service, Santa Fe, New Mexico. (Available from: https://irma.nps.gov/DataStore/Reference/Profile/2305190)

Pathak, V., and V. V. Sugunan. 1980. Effect of solar eclipse on the photosynthetic processes and behavior of biotic communities in a Nagarjunasagar India aquatic ecosystem. Journal of the Inland Fisheries Society of India 12:121–126.

Ritson, R., D. H. Ranglack, and N. Bickford. 2019. Comparing social media observations of animals during a solar eclipse to published research. Animals 9:59.

Savoy, P., E. Bernhardt, L. Kirk, M. J. Cohen, and J. B. Heffernan. 2021. A seasonally dynamic model of light at the stream surface. Freshwater Science 40:286–301.

Savoy, P., and J. W. Harvey. 2021. Predicting light regime controls on primary productivity across CONUS river networks. Geophysical Research Letters 48:e2020GL092149.

Shapiro, S. S., and M. B. Wilk. 1965. An analysis of variance test for normality (complete samples). Biometrika 52:591–611.

Simino, J. 2002. East Fork Jemez River stream inventory report. Santa Fe National Forest, United States Department of Agriculture Forest Service, Santa Fe, New Mexico. (Available from: https://www.fs.usda.gov/detail/santafe/landmanagement/resourcemanagement/?cid=fsbdev7_021021)

Skud, B. E. 1967. Responses of marine organisms during the solar eclipse of July 1963. United States Fish and Wildlife Service, Bureau of Commercial Fisheries Biological Laboratory, Boothbay Harbor, Maine, Fishery Bulletin 66:259–271. (Available from: https://spo.nmfs.noaa.gov/sites/default/files/pdf-content/fish-bull/skud_0.pdf)

Sokal, R. R., and F. J. Rohlf. 1969. Biometry. The principles and practice of statistics in biological research. W. H. Freeman and Company, San Francisco, California.

Summers, B. M., D. J. Van Horn, R. González-Pinzón, R. J. Bixby, M. R. Grace, L. R. Sherson, L. J. Crossey, M. C. Stone, R. R. Parmenter, T. S. Compton, and C. N. Dahm. 2020. Long-term data reveal highly variable metabolism and transitions in trophic status in a montane stream. Freshwater Science 39: 241–255.

Suter, P. J., and W. D. Williams. 1977. Effect of a total solar eclipse on stream drift. Australian Journal of Marine and Freshwater Research 28:793–798.

USGS [United States Geological Survey]. 2011. Change to solubility equations for oxygen in water. Office of Water Quality Technical Memorandum 2011.03. (Available from: https://water.usgs.gov/water-resources/memos/documents/WQ.2011.03.pdf)

Van Horn, D. J., C. S. White, E. A. Martinez, C. Hernandez, J. Merrill, R. R. Parmenter, and C. N. Dahm. 2012. Linkages between riparian characteristics, ungulate grazing, and geomorphology and nutrient cycling in montane grassland streams. Journal of Rangeland Ecology and Management 65:475–485.

Vecchione, M., R. S. Maples, and R. Donahoe. 1986. Changes in chlorophyll a concentration in a shallow water column during a solar eclipse. Smithsonian Contributions to the Marine Sciences 29:37–44.